JOURNAL OF OPTOELECTRONICS AND ADVANCED MATERIALS Vol. 9, No. 10, October 2007, p. 3194 - 3199

Thermally induced changes on the electrical and optical properties of nanocrystalline CdSe thin films

JEEWAN SHARMA, G. S. S. SAINI, N. GOYAL, S. K. TRIPATHI*
Department of Physics, Centre of Advanced Study in Physics, Panjab University, Chandigarh-160 014, India

The present paper reports the electrical and optical properties on nanocrystalline CdSe (n-CdSe) thin films before and after thermal treatment. The absorption coefficient (α) and band gap (E_g) are calculated using transmission curves. The crystallite size is calculated using XRD and also from the measured band gap shift with respect to bulk value. The dark conductivity (σ_d) measurements indicate that the conduction in this material is through an activated process having single activation energy in the investigated temperature range (253–370 K). Steady state photoconductivity (σ_{ph}) measurements are done as a function of temperature and intensity. Results show that the above properties change drastically after the thermal treatment.

(Received July 3, 2007; accepted October 1, 2007)

Keywords: CdSe thin films, Nanocrystalline, Optical properties, Photosensitivity, Photoconductivity

1. Introduction

In recent years, there has been an increasing interest in the area of nanophase materials, which encompasses structures such as nanoclusters, quantum dots etc. [1–3]. Low dimensional materials are an exciting class of materials whose properties lie between those of atomic/ molecular clusters and bulk materials. Reduction in particle size leads to changes in the electronic structure, thereby, influencing the density of states (DOS). A key aspect of semiconductors in a nanocrystalline thin film form is the modification of the energy levels and the density of states owing to the confinement of the charge carriers. The charge carriers are localized in nanocrystals and this leads to a blue shift in the band gap [4,5]. Semiconductor nanoparticles exhibit size-dependent electronic band gap energies [6], melting temperatures [7], soild-solid phase transition temperatures [8] and pressures [9]. It is important for such systems to have useful luminescence as well as photoconductivity characteristics, which can then be tailored through size control.

CdSe is well known as a very good photoconducting material. It has been investigated for many years for its potential applications in electrography, photoconducting and photovoltaic cells, thin film transistors and lasers [10]. The use of CdSe in photoconductivity results in detectors with a faster response than CdTe photodetectors. CdSe films have been used to fabricate photoelectrochemical (PEC) cells with higher efficiency [11–13]. Simulations indicate that about 30% efficiency can be achieved with a four-terminal thin-film tandem structure using CdSe [14]. The properties of nanomaterials are critically dependent on the nature of preparation technique and subsequent heat treatments like annealing in air, vacuum or different gaseous environments like H_2, Ar, N_2 etc [15].

The present paper reports the effect of annealing in vacuum, on the properties of n-CdSe thin films deposited by inert gas condensation method using Ar as carrier gas. n-CdSe thin films have been deposited at a partial pressure of 2×10^{-1} mbar and room temperatures (298 K). Optical measurements have been taken at room temperature and the different parameters like absorption coefficient (α) and band gap (E_g) have been calculated. The steady state photoconductivity is studied as a function of temperature (253-370 K) at intensity 8450 Lux. The intensity dependence of the photoconductivity is studied at 298 K. Section 2 describes the experimental details. The results have been presented and discussed in section 3. The last section deals with the conclusions of this work.

2. Experimental procedure

The semi conducting $Cd_{30}Se_{70}$ was prepared from its constituents (5N pure) by melt-quenching technique as described earlier [16]. Thin films of this material were prepared in a conventional vacuum coating system on well degassed Corning 7059 glass substrates. Before the deposition, the substrates were cleaned chemically. Then these were heated at 120 ^oC to remove any moisture or methanol present. The vacuum chamber was evacuated to 2×10^{-6} mbar before the deposition. The Ar gas was introduced into the chamber through specially designed inlet tube having a jet of diameter ~ 0.5 mm. This jet was kept adjacent to the evaporation boat pointing towards the glass substrates. The vacuum chamber was purged several times with spectroscopic grade Ar gas to remove any residual gas impurities. Thermal evaporation of the material was carried out from the Mo boat. Finally, CdSe was evaporated at Ar gas pressure of 2×10^{-1} mbar and 298 K. The distance between the source and the substrate was

about 7 cm. This film is then annealed at 473 K for one hour. Annealing is done in vacuum of ~ 2×10^{-3} mbar.

Crystallographic study was carried out before and after annealing using a Phillips PW-1710 X-ray diffractometer using CuK_α radiation in the 2θ range from 10° to 70°. To study the optical properties of n-CdSe thin films, the transmission spectra were recorded using Monochromator-spectrograph [*SOLAR TII*, MS 2004] in the transmission range 400-1000 nm for all samples. The electrical measurements of these thin films were carried out in a specially designed metallic sample holder where heat filtered white light of intensity 8450 Lux (200 W tungsten lamp) was shown through a transparent glass window. A vacuum of about 10^{-3} mbar was maintained throughout these measurements. Light intensity was measured using a digital luxmeter (*MASTECH*, MS6610). Planar geometry of the films (length ~ 1.0 cm; electrode gap 8×10^{-2} cm) was used for the electrical measurements. Thick In electrodes were used for the electrical contacts. The film thickness was measured to be ~ 100 nm with the commonly used weight difference method. The photocurrent (I_{ph}) was obtained after subtracting the dark current (I_d) from the current measured in the presence of light. The dark- and photo- current was noted manually using a digital picoammeter (DPM-11 Model). The accuracy in I_{ph} measurements was typically 1 pA.

3. Results and discussion

3.1 Structural and Optical Properties

The spectrum in Fig. 1 (i) shows the diffraction spectrum of n-CdSe thin film before (as-deposited) and after annealing. In as-deposited film there is a highest intensity reflection peak at $2\theta = 25.3^\circ$ [111], with two small another intensity peaks at $2\theta = 41.8^\circ$ [220] and 49.5° [311]. Some new peaks at $2\theta = 24.1^\circ$ [100], 27.4° [101], 35.4° [102] and 45.9° [103] are observed for the annealed film and the intensity of peaks is increased after annealing. The broad hump in the background [Fig. 1 (i) (a)] is due to the amorphous glass substrate and also due to some amorphous phase present in the n-CdSe thin film. The comparison of observed 'd' values with standard 'd' values [17,18] confirms that the as-deposited film is having sphalerite cubic (zinc blende type) nanocrystalline structure while the new peaks in annealed film are due to hexagonal phase present in it.

Information of the strain and the particle size are obtained from the full width at half maximum (FWHMs) of the diffraction peaks. The FWHMs (β) can be expressed as a linear combination of the contributions from the strain (ε) and particle size (L) through the following relation [19]

$$\frac{\beta\cos\theta}{\lambda} = \frac{1}{L} + \frac{\varepsilon\sin\theta}{\lambda} \qquad (1)$$

Fig. 1 (ii) represents the plots of $(\beta\cos\theta)/\lambda$ versus $(\sin\theta)/\lambda$ for both films which are straight lines. The slope of the plots gives the amount of residual strain, which turns out to be -8.13×10^{-2} and 6.39×10^{-3} for as-deposited and annealed films. The reciprocal of intercept on the $(\beta\cos\theta)/\lambda$ axis gives the average particle size as ~ 3.9 nm and 20.8 nm respectively. The increase in the particle size from 3.9 nm to 20.8 nm with annealing shows the improvement in the crystallinity of the film. The negative value of residual strain for the as-deposited film indicates the compressive strain. The annealed film has positive value of residual strain indicating the strain in this film is tensile. If the film is deposited free from impurities, the compressive strain is generated at the thin film substrate interface, when the very small crystallites are bonded to substrates due to surface tension effect.

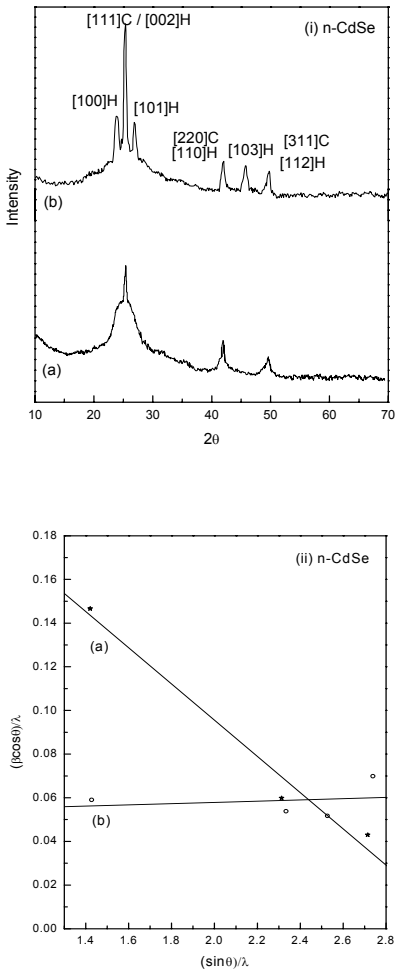

Fig. 1. (i) XRD patterns and (ii) Size and strain analysis plots for (a) as-deposited and (b) annealed n-CdSe thin films.

Optical properties are studied by recording the transmission spectra of the films. From the transmission data, nearly at the fundamental absorption edge, the values of absorption coefficient (α), are calculated in the region of strong absorption using the relation:

$$\alpha = \frac{1}{d}\ln\left(\frac{1}{T}\right) \tag{2}$$

The fundamental absorption, which corresponds to the transition from valence band to conduction band, can be used to determine the band gap of the material. The relation between α and the incident photon energy ($h\nu$) can be written as [20]

$$\alpha = \frac{A\left(h\nu - E_g\right)^n}{h\nu} \tag{3}$$

where A is a constant, E_g is the band gap of the material and the exponent n depends on the type of transition. The n may have values 1/2, 2, 3/2 and 3 corresponding to the allowed direct, allowed indirect, forbidden direct and forbidden indirect transitions, respectively.

Table 1. Representation of strain, particle size and band gap for as-deposited and annealed n-CdSe thin films.

Film	Strain	Particle size (nm)		Band Gap
		XRD	Optical	(eV)
As-deposited	-8.13×10^{-2}	03.9	2.24	(2.22 ± 0.01)
Annealed	6.39×10^{-2}	20.8	3.61	(1.90 ± 0.01)

In case of nanocrystalline films, there may be some deviation from a bulk like transition. Now Eq. (3) may be written as

$$\frac{d\{\ln(\alpha h\nu)\}}{d(h\nu)} = \frac{n}{(h\nu - E_g)} \tag{4}$$

The above equation indicates that the plot of d{ln($\alpha h\nu$)}/d($h\nu$) vs $h\nu$ must have a divergence at an energy value equal to E_g, where the transition takes place.

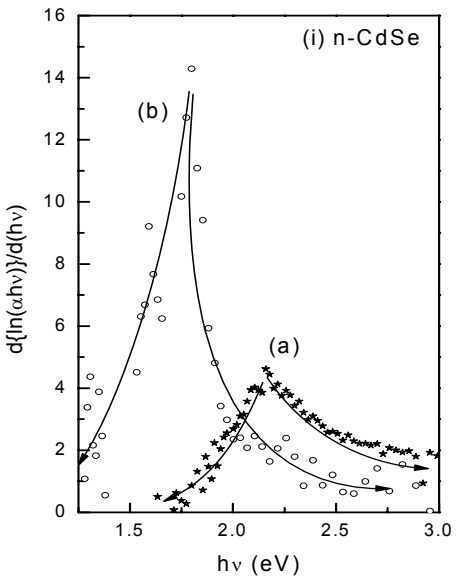

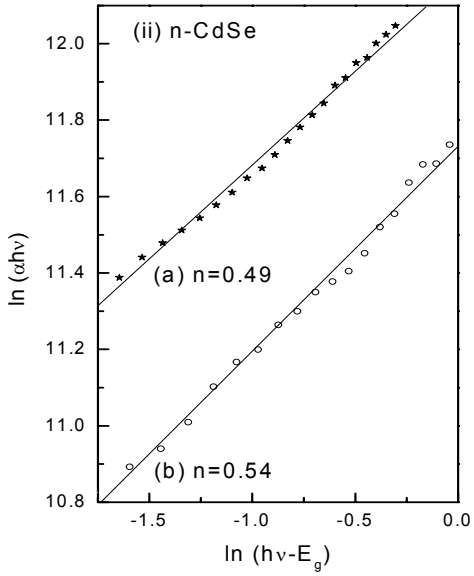

Fig. 2. (i) Variation of d{ln(αhν)}/d(hν) with energy and (ii) plots of ln (αhν) vs ln ($h\nu - E_g$) for (a) as-deposited and (b) annealed n-CdSe thin films.

Fig. 2 (i) shows the plots of d{ln($\alpha h\nu$)}/d($h\nu$) vs $h\nu$ for as-deposited and annealed films, with discontinuity at 2.18 eV and 1.80 eV respectively. Taking these values as the optical gap of n-CdSe thin films, ln ($\alpha h\nu$) vs ln ($h\nu - E_g$) graphs are plotted. From the slope of these straight line graphs [Fig. 2 (ii)], value of n has been calculated to be 0.49, and 0.54 respectively, which are close to 0.5 indicating that the transition is direct. The value of optical gap is calculated by extrapolating the straight line portion of $(\alpha h\nu)^{1/n}$ vs $h\nu$ graph to $h\nu$ axis taking n = 0.5. Fig. 3 shows the plots of $(\alpha h\nu)^2$ vs $h\nu$ for as-deposited and annealed thin films. The correct values of the optical gap

calculated from the figure are (2.22 ± 0.01) eV and (1.90 ± 0.01) eV for as-deposited and annealed thin films. The value of optical gap is found to decrease after annealing. These values of optical gap are inserted in Table 1. Clearly, the observed values of E_g are higher than the value of bulk optical gap of CdSe [(1.74 ± 0.01) eV] [21] due to quantum confinement in the CdSe nanocrystallites.

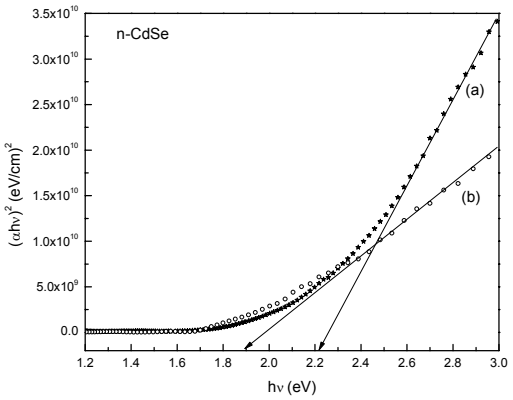

Fig. 3. Variation of $(\alpha h\nu)^2$ with energy for (a) as-deposited and (b) annealed n-CdSe thin films.

From the blue-shift of the band gap (E_g), we can calculate the average diameter of the particles using relation [22,23], since change in the value of E_g suggests weak confinement of the exciton:

$$\Delta E_g = E_g(film) - E_g(bulk) = E_{shift} = \frac{\hbar^2 \pi^2}{2\mu R^2} \qquad (5)$$

where E_{shift} is the shift in the band gap, μ the translation mass (m_{hole} + $m_{electron}$) and R the radius of the nanoparticles. This formula is applicable in our case as we are well below the strong confinement regime and hence observe the effects due to weak confinement of the exciton only. We have calculated the average diameter of the particles using Eq. (5) as ~ 2.24 nm and 3.61 nm for as-deposited and annealed n-CdSe thin films respectively. These values do not agree with the calculated values from the XRD data (Table 1). Infact, the experimentally measured crystalline size in the small size regime does not agree well with the size estimated from the blue shift using effective mass approximation [24]. The disagreement in size estimated by XRD and the blue shift can be assigned, therefore, to the non-spherical geometry of nanoparticles.

3.2 Electrical Properties

Fig. 4 (i) shows the temperature dependence of dark conductivity (σ_d) for as-deposited and annealed n-CdSe thin films in the temperature range 253-370 K.

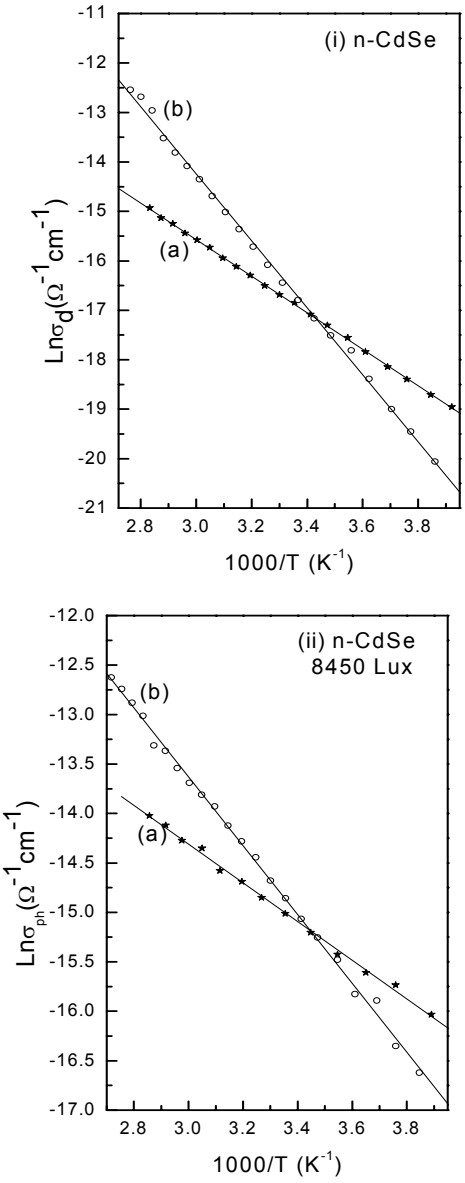

Fig. 4. Temperature dependence of (i) dark conductivity and (ii) photo conductivity for (a) as-deposited and (b) annealed n-CdSe thin films.

The electrical conductivity shows typical Arrhenius type of activation

$$\sigma_d = \sigma_o \exp\left(\frac{-\Delta E}{kT}\right) \qquad (6)$$

where ΔE is the activation energy for conduction and k is the Boltzmann's constant. The values of σ_d, calculated using Eq. (6), are (4.62 ± 0.02)×10^{-8} Ω^{-1}cm^{-1} and (7.23 ± 0.02)×10^{-8} Ω^{-1}cm^{-1} for as-deposited and annealed n-CdSe thin films respectively. The value of σ_d increases as the particle size of n-CdSe increases. The increase in

conductivity after annealing in these films is attributed to the improvement in crystallite size of films [15,25]. The increase in electrical conductivity and activation energies after annealing may be due to the change in structural parameters, improvement in crystallite and grain size, decrease in inter-crystallite boundaries (grain boundary domains) and removal of some impurities (adsorbed and absorbed gases). Excess atoms of compound are also possible [26] due to a small change in stoichiometry after annealing. Fig. 4 (ii) shows the temperature dependence of photoconductivity (σ_{ph}) for as-deposited and annealed thin films. The values of σ_{ph}, calculated using Eq. (6), are found to be $(2.93 \pm 0.02)\times10^{-7}$ $\Omega^{-1}cm^{-1}$ and $(4.22 \pm 0.02)\times10^{-7}$ $\Omega^{-1}cm^{-1}$ for as-deposited and annealed thin films respectively. The photo activation energy (ΔE_{ph}) has been calculated using the slopes of Fig.4 (ii) and are inserted in the Table 2. The value of σ_{ph} increases on annealing of n-CdSe thin film. The activation energy for photoconduction is much smaller than dark conduction. No maximum in the steady state photoconductivity with temperature has been observed in the measured temperature range. Photosensitivity (σ_{ph}/σ_d) is found to decrease after annealing.

Intensity (F) dependence of steady state photoconductivity has also been studied to see the nature of recombination processes in all samples. The plot of $\ln\sigma_{ph}$ vs $\ln F$ are straight lines (result not shown), indicating that σ_{ph} follows a power law with F, i.e. $\sigma_{ph} \propto F^{\gamma}$, with $0.5 \le \gamma \le 1.0$. According to Rose [27], the value of γ between 0.5 and 1.0 can not be understood by assuming a set of discrete trap levels but considering the existence of continuous distributions of trap levels in the band gap. In as-deposited and annealed thin films, the values of γ are found to be in between 0.5 and 1.0, which indicate that continuous distribution of localized states exists in the mobility gap of the present materials and the resulting recombination mechanism is bimolecular [27], where the recombination rate of electrons is proportional to the number of holes.

Table 2. Representation of dark-, photo-conductivity, dark-, photo-activation energy, γ and photosensitivity for as-deposited and annealed n-CdSe thin films.

Film	σ_d (Ω^{-1} cm^{-1})	σ_{ph} (Ω^{-1} cm^{-1})	ΔE_d (eV)	ΔE_{ph} (eV)	γ	σ_{ph}/σ_d
As-deposited	$(4.62 \pm 0.02)\times10^{-8}$	$(2.93 \pm 0.02)\times10^{-7}$	(0.31 ± 0.01)	(0.17 ± 0.01)	0.51	6.34
Annealed	$(7.23 \pm 0.02)\times10^{-8}$	$(4.22 \pm 0.02)\times10^{-7}$	(0.58 ± 0.01)	(0.30 ± 0.01)	0.58	5.81

4. Conclusions

As-deposited and annealed CdSe thin films are nanocrystalline in nature. As-deposited film is found to have sphalerite cubic nanocrystalline structure while hexagonal character starts increasing when films annealed in vacuum at 473 K for one hour. The particle size increases from 3.9 nm to 20.8 nm (XRD) after annealing. The strain is found to decrease from -8.13×10^{-2} to 6.39×10^{-3} after annealing. The strain in as-deposited film is compressive while annealed film is having tensile strain. A blue shift in the fundamental edge has been observed which may be due to the confinement effects. There is a blue shift of 0.48 eV and 0.16 eV as-deposited and annealed n-CdSe thin films respectively. The values of particle size calculated from blue shift are found to increase from 2.24 nm to 3.61 nm respectively. The value of σ_d and ΔE_d increases as the particle size of n-CdSe increases. Steady state photoconductivity studies indicate that there is continuous distribution of localized states.

Acknowledgements

This work is financially supported by the C.S.I.R. (Major Research Project), New Delhi.

References

[1] S. Lee, D. Song, D. Kim, J. Lee, S. Kim, I.Y. Park, Y.D. Choi, Mat. Letts. **58**, 342 (2004).
[2] V.P. Kochereshko, A.V. Platonov, A.S. Gurevich, Journal of Luminescence, **125**, 133 (2007).
[3] A. Crunteanu, F. Dumas-Bouchiat, C. Champeaux, A. Catherinot, P. Blondy, Thin Solid Films **515**, 6324 **(**2007).
[4] U.V. Desnica, I.D. Desnica-Frankovic, O. Gamulin, C.W. White, E. Sonder, R.A. Zuhr, J. Non-Cryst. Solids **299**, 1100 (2002).
[5] L Li, J. Hu, W. Yang, A.P. Alivisatos, Nano Letters **1**, 349 (2001).
[6] L.E. Bruce, J. Chem. Phys. **80**, 4403 (1984).
[7] Z. Zhang, M. Zhao, Q. Jiang, Semicond. Sci. Technol. **16**, L33 (2001).
[8] S.B. Qadri, E.F. Skelton, D. Hsu, A.D. Dinsmore, J. Yang, H.F. Gray, B.R. Ratna, Phys Rev. B **60**, 9191 (1999).
[9] C.C. Chen, A.B. Herhold, C.S. Johnson, A.P. Alivisatos, Science **276**, 398 (1997).
[10] D. Samanta, B. Samanta, A.K. Chaudhuri, S. Ghorai, U. Pal, Semicond. Sci. Technol. **11**, 548 (1996).
[11] S.J. Lade, M.D. Uplane, C.D. Lokhande, Mater. Chem. Phys. **68**, 36 (2001).

[12] M.A. Russak, S.K. Dev, J. Electrochem. Soc. **127**, 725 (1980).
[13] M.T. Gutierrez, J. Ortega, J. Electrochem. Soc. **136**, 2316 (1989).
[14] P. Mahawela, S. Jeedigunta, S. Vakkalanka, C.S. Ferekides, D.L. Morel, Thin Solid Films **480-481**, 466 (2005).
[15] R.B. Kale, C.D. Lokhande, Applied Surface Science **223**, 343 (2004).
[16] J. Sharma, G. Singh, A. Thakur, G.S.S. Saini, N. Goyal, S.K. Tripathi, J. Optoelectron. Adv. Mater. **7**, 2085 (2005).
[17] JCPDS Data File No. 8-459.
[18] JCPDS Data File No. 19-191.
[19] S.B. Qadri, E.F. Skelton, D. Hsu, A.D Dinsmore, J. Yang, H.F. Gray, B.R. Ratna, Phys. Rev. B **60**, 9191 (1999).
[20] J.I. Pankove, Optical Processes in Semiconductors, Englewood Cliffs. NJ: Prentice-Hall (1971).

]

[21] A. Gaur, D.K. Sharma, D.S. Ahlawat, N. Singh, J. Opt. A: Pure Appl. Opt. **9**, 260 (2007).
[22] Al.L. Efros, A.L. Efros, Sov. Phys. Semicond. **16**, 772 (1982).
[23] W. Wei-Yu, J.N. Schulman, T.Y. Hsu, F. Uzi, Appl. Phys. Lett. **51**, 710 (1987).
[24] Y. Wang, A. Suna, W. Mahler, R. Kasowski, J. Chem. Phys. **87**, 7315 (1987).
[25] S. Velumani, S.K. Narayandass, D. Mangalaraj, Semicond. Sci. Technol. **13**, 1016 (1998).
[26] S. Ghosh, A. Mukherjee, H. Kim, C. Lee, Materials Chemistry and Physics **78**, 726 (2003).
[27] G.I. Rusu, M.E. Popa, G.G. Rusu, I. Salaoru, Applied Surface Science **218**, 222 (2003).

*Corresponding author: surya@pu.ac.in;
surya_tr@yahoo.com